Materials Science and Engineering C 79 (2017) 93–99

Contents lists available at ScienceDirect

Materials Science and Engineering C

journal homepage: www.elsevier.com/locate/msec

Carbon nanotube ensembled hybrid nanocomposite electrode for direct electrochemical detection of epinephrine in pharmaceutical tablets and urine

K. Koteshwara Reddy [a,b], M. Satyanarayana [a], K. Yugender Goud [a], K. Vengatajalabathy Gobi [a], Hern Kim [b,*]

[a] Department of Chemistry, National Institute of Technology, Warangal, Telangana 506004, India
[b] Department of Energy Science and Technology, Smart Living Innovation Technology Center, Myongji University, Yongin, Gyeonggi-do 17058, Republic of Korea

ARTICLE INFO

Article history:
Received 1 December 2016
Received in revised form 24 April 2017
Accepted 4 May 2017
Available online 4 May 2017

Keywords:
Epinephrine
Carbon nanotubes
Chitosan
Raman spectroscopy
Electrochemical biosensor
Artificial urine

ABSTRACT

An efficient electrochemical sensor for selective detection of the neurotransmitter, epinephrine (Epn), has been fabricated with the aid of a functionalized multiwall carbon nanotube–chitosan biopolymer nanocomposite (*Chit-fCNT*) electrode. Multiwall carbon nanotubes (CNT) were successfully functionalized with the aid of nitric acid and confirmed by the Raman spectral data. Functionalized carbon nanotubes (*fCNT*) were dispersed in chitosan solution and the resulting bio-nanocomposite was used for the fabrication of sensor surface by drop and cast method. Electrochemical characteristics of the fabricated sensor were understood using cyclic, differential pulse voltammetry (CV, DPV) and electrochemical impedance analysis for the detection of Epn in phosphate buffer (pH 7.4). CV and impedance analysis revealed that the *Chit-fCNT* modified electrode enhances the electrodic reaction of Epn and facilitated the electron transfer more readily compared to that of bare electrode. Applying DPV for the detection of Epn, achieved 30 nM as the lowest detection limit in the determination range of 0.05–10 μM and the analytical time as low as 10 s. Selective determination of Epn against the coexistence of a number of biological electroactive interferents and reproducible results for the determination of Epn were demonstrated. The present biosensor has been found efficient for successful direct determination of Epn from pharmaceutical adrenaline formulations and urine samples.

1. Introduction

Epinephrine (Epn), the neurotransmitter, is present in human serum at about nM levels. Epn was first isolated in 1901 and synthesized in 1904 [1]. Epn is crucial for the successful performance of cardiovascular and central nervous systems. Several physiological phenomena are correlative to Epn levels in biological fluids and its measurement is a key factor in the medical diagnosis of diabetes, Parkinson's disease and cerebral malaises [2]. Epn is the most prescribed common emergency healthcare medicine. Recent literature reports reveal that World Anti-Doping Agency (WADA) has banned Epn usage during competitive games [3].

A simple, highly selective and rapid detection of Epn in both physiological fluids and pharmaceutical samples is highly necessitated. Quantitative analysis of Epn is essential in the development of physiological investigations, pharmacological research and life science. Detection and quantification of Epn has been reported by various methods such as absorbance, fluorescence, capillary electrophoresis [4], electrochemiluminescence [5], HPLC [6] and chromatography coupled with mass spectrometry [7–9]. However, these methods suffer from either tedious procedure or low sensitivity. Therefore, a simple and convenient method needs to be developed for Epn detection.

Electrochemical techniques can be employed for the successful quantification of Epn as it can undergo oxidation very easily. But, the electrochemical detection of Epn at bare electrodes involves various basic difficulties, mainly *high overpotential* and *sluggish kinetics of electrodic processes*, which result in insignificant electrochemical responses. Another major problem is the coexistence of Epn with other electroactive biological compounds such as ascorbic or uric acid which would also undergo oxidation at unmodified electrodes at almost the same potentials. So, it is necessary to overcome the electrodic reaction of these interferents to achieve a selective determination of Epn [10].

Selective and rapid detection of Epn despite the coexistence of various potential biological interferents is an important target of electroanalytical research. To overcome these drawbacks, extensive research investigations were dedicated by scientists to develop new surface modified electrodes which eliminate possible interventions from the potential interferents [11]. Wide range of molecular recognition elements were reported in developing highly selective recognition matrices for neurotransmitters. Biomolecules (antibodies, nucleic acids, aptamers and dendrimers), self-assembled monolayers, mesoporous

* Corresponding author.
E-mail address: hernkim@mju.ac.kr (H. Kim).

http://dx.doi.org/10.1016/j.msec.2017.05.012
0928-4931/

materials, sol-gel derivatives, molecular imprinted polymers and conducting polymers have been investigated as recognition matrices [12]. Nanoparticles of noble metals, other metals and non-metals [13–16] can be used in the fabrication of inorganic recognition matrices. Further, the combination of metal nanoparticles with other functional materials steers to the advanced hybrid nanomaterials which possess unique and distinct characteristics. Hybrid core-shell nanostructures [17], metal nanoparticle-hydrogel composites [18], nanoparticle-polymeric hybrid scaffolds [19–21], metal nanoparticle-biomolecule bioconjugates [22,23], anisotropic Janus particles [24] and carbon dots [25] can offer advantages in the fabrication of recognition matrix.

Unique characteristic properties of carbon nanotubes (CNT) offer wide range of applications in innumerable fields. High electrical conductivity and long nanowire-like structure of CNT have attracted for the fabrication of highly sensitive electrochemical sensors. CNT could reduce electrode fouling and thus could promote improved reuse of CNT based electrodes. But, the prime drawback of CNT is their low solubility in majority of the solvents. Several strategies have been proposed to enhance the CNT dispersion in polymer electrolytes, ionic liquids, biopolymer matrices and intercalation with polymers and composite matrices [9,26].

Chitosan (Chit) is a β-linked polysaccharide with remarkable biocompatibility and biodegradability and is extracted from the natural abundant chitin by partial deacetylation. Chit comprises unique characteristic properties such as excellent film forming, adherence, stability and numerous reactive amino and hydroxyl groups for functionalization [27]. In this work, a stable and uniform CNT–Chit nanocomposite film was achieved using Chit.

In the present study, we fabricated an electrochemical biosensor for Epn employing *Chit-fCNT* nanocomposite for the modification of electrode surface. Functionalization of CNT was confirmed using Raman spectroscopy. Morphological characteristics of the nanocomposite film were explored using scanning electron microscopic (SEM) analysis. Electrocatalytic activity and selectivity of the *Chit-fCNT* nanocomposite modified electrode towards the detection of Epn were investigated with cyclic, differential pulse voltammetry (CV, DPV) and electrochemical impedance spectroscopy (EIS) techniques. Feasibility for the direct determination of Epn selectively from pharmaceutical adrenaline injections and artificial urine samples was established.

2. Experimental

2.1. Materials

Epinephrine, ascorbic acid, uric acid, serotonin and chitosan (low molecular weight biopolymer of ~60 kDa from crab shells and ~85% deacetylated) were bought from Sigma (USA). Multiwall carbon nanotubes of 20–50 nm diameter and 2–5 μm length were received from Sisco Research Laboratories Pvt. Ltd. (India). Chemicals used for the preparation of buffers and artificial urine samples were analytical grade with a minimum of 99% purity. Pharmaceutical samples of epinephrine (Vasocon injection, 1 mg mL^{-1} adrenaline bitartrate) were received from the dispensary of our Institute. All the aqueous buffer and electrolyte solutions were prepared with double-distilled deionized water of high resistance (18 MΩ) which passed through a 0.2 μm Whatman filter. Phosphate buffer solution (PBS, 50 mM) was prepared by adding appropriate quantities of K_2HPO_4 and KH_2PO_4 as explained in the Sigma-Aldrich product information, and the anticipated pH was acquired by the addition of 0.1 M NaOH. Artificial urine samples of pH 7.4 were prepared as mentioned in the reported literature [28].

2.2. Functionalization of carbon nanotubes

Multiwall carbon nanotubes (CNT) were treated with nitric acid to bring in functional carboxyl groups according to the procedure [29] with minor modifications as follows. 120 mg of CNT were introduced to 10 mL aq. 3 N nitric acid, then maintained at ~70 °C for 24 h under constant stirring. Nitric acid oxidizes and introduces carboxyl groups at the sidewall defects and edges of the nanotubes. After the treatment, the black solid compound was centrifuged, separated, and then cleaned with water several times so that the supernatant becomes neutral. Functionalized CNT (*fCNT*) was dried at 80 °C for 12 h.

2.3. Electrode modification by fCNT hybrid nanocomposite

At first, fresh surface of glassy carbon electrodes (GCE, 3 mm diameter) was obtained by polishing with alumina slurries of 3 μm and moving down to 0.05 μm, and the electrodes were then cleaned in 1:2 v/v dil.HNO_3, ethanol and water by ultrasonication for 3 min each. Chitosan was dispersed in aq. 1% (v/v) acetic acid solution at 1% (w/v) concentration. Functionalized CNT was dispersed into the chitosan solution at 4 mg mL^{-1} concentration by using ultrasonication for ~10 min. Freshly polished GCE surface was modified using 8 μL of the dispersion of *fCNT* by drop-cast method and the resultant electrode is denoted as *GCE/Chit-fCNT*.

2.4. Analytical methods

Electrochemical measurements (CV, DPV) were performed in a two-compartment cell using a CHI-619D analyzer (CH Instruments, USA) at room temperature with bare or modified GCE as working electrode, a Pt spiral wire as counter electrode and an Ag/AgCl (3 N KCl) electrode as reference electrode. EIS response was investigated using Zahner-IM6e workstation (Germany) in 10 mHz–100 KHz frequency range with 10 mV excitation amplitude and 64 as sine wave count. Electrolyte contents were deaerated with nitrogen gas for 15 min prior to each electrochemical analysis and continuously maintained the flow of nitrogen over the electrolyte surface.

SEM analysis was carried out using SEM-TESCAN, VEGA 3 LMU model for analyzing morphology of *Chit-fCNT* nanocomposite. Sample was prepared by the dispersion of 4 mg mL^{-1} *fCNT* in 1% (w/v) Chit solution. A small volume (~5 μL) of the dispersion was casted on to the carbon tape supported on SEM sample stub. The sample was sputtered for 60 s with gold using a mini sputter coater (QUORUM Technologies, SC7620). Raman vibrational spectra of MWCNT samples were recorded with LabRAM (HR800 model, France) spectrometer; a He-Ne (633 nm) laser of 20 mW power has been employed with 5× objective and the samples were dispersed in 4:1 (v/v) acetonitrile:methanol mixture.

3. Results and discussion

3.1. Raman spectra of CNT and fCNT

Pristine- and functionalized-CNT were characterized by Raman spectroscopy. Both pristine CNT and *fCNT* exhibit four characteristic peaks namely D, G, D′ and D* bands in their Raman spectral data (Fig. 1). The characteristic peak at ~1330 cm^{-1} is relevant to the defect derived D band which represents the defect sites or disordered graphitic structure of CNT. The peak at ~1580 cm^{-1} is assigned as graphitic structure derived G band which represents the >C=C< bond nature in the graphitic plane of CNT. Raman vibrational peak at ~1610 cm^{-1} represents D′ band which indicates the defective sites in the manufacture of CNT. The vibrational peak at ~2660 cm^{-1} (D*) is the overtone of D band originated from a double-resonance process [30–32]. Relatively smaller D band indicates high purity of CNT whereas larger D band is likely due to the influence of terminal groups or defect sites. Quality of CNT could be decided based on the ratio of these peak intensities, in other words I_D/I_G values would be considered in determining the purity of CNT. When compared the I_D/I_G values of *fCNT* (1.4594) with that of pristine CNT (1.1824), the increment in I_D/I_G value of *fCNT* suggests that the formation of some sp^3 carbons by oxidation in the case of

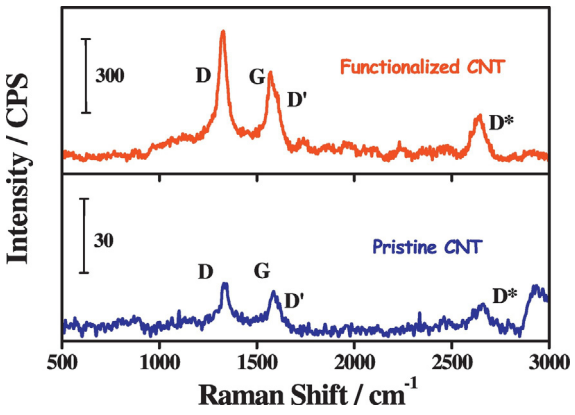

Fig. 1. Raman vibrational spectra of pristine and functionalized CNT.

fCNT, which confirms the successful functionalization of CNT with –COOH groups [26,33,34].

3.2. Surface morphology and active surface area of Chit-fCNT composite electrodes

Determination of electroactive area of bare and *Chit-fCNT* nanocomposite modified electrodes was explained in detail in our previous report [35]. Based on the Randles-Sevcik equation and CV experiments, the electroactive area of bare GCE was observed as 0.071 cm^2, whereas 0.262 cm^2 for *GCE/Chit-fCNT*. This result reveals the efficient dispersion of nanostructured *fCNT* in the biopolymer matrix of Chit, which increased the electroactive area when compared to bare GCE.

SEM analysis was carried out for understanding the morphological features of *Chit-fCNT* matrix. SEM images of *Chit-fCNT* film casted on a carbon tape are shown in Fig. 2 at two different magnifications. The SEM images disclose individual, discrete and well-dispersed thread-like structures of *fCNT* all throughout the surface (Fig. 2) with porous nature, which would have increased the active area of *GCE/Chit-fCNT*. Dispersing nature of Chit and the nanostructured *fCNT* both acted concomitantly in enhancing the active surface area of *GCE/Chit-fCNT* [36].

3.3. Electrocatalytic oxidation of epinephrine

CV analysis of 0.1 mM epinephrine was carried out in 50 mM PBS (pH = 7.4) with a potential scan rate of 100 mV s^{-1}. Epn oxidized irreversibly in the defined potential window exhibiting an anodic peak at +170 mV with *GCE/Chit-fCNT* and at +315 mV with bare GCE. Both bare and modified electrodes did not show any characteristic peak in blank PBS. Interestingly, the anodic peak of Epn was altered towards less positive potential region by ~140 mV at *GCE/Chit-fCNT*, and this reduction in overpotential is the added advantage observed with the fabricated electrode besides the increase in peak current by ~2 times in the case of *Chit-fCNT* modified electrode compared to that of bare GCE. The enhanced peak currents can be ascribed to the high surface area, porous nature of the nanocomposite film and unique structural morphology of *fCNT*. Nature of the electrochemical oxidation of Epn was studied with different scan rates at *GCE/Chit-fCNT* in 0.1 mM Epn. Cyclic voltammograms show gradual increment in the oxidation peak current when the scan rate increased from 10 to 200 mV s^{-1}. The plot of anodic peak current against the square root of scan rate ($\nu^{1/2}$) is shown in Fig. 3(B). The plot was a straight line passing through the origin, inferring that the electrodic reaction of Epn at *GCE/Chit-fCNT* as a diffusion controlled phenomenon.

3.4. Electrochemical impedance analysis

EIS offers a better understanding of the interfacial characteristics of any surface-modified electrode. EIS analysis is represented in both Nyquist and Bode plot formats. In the Nyquist plot, semi-circle behavior represents charge-transfer phenomena (oxidation or reduction or simple electron transfer) and the straight line with 45° slope suggests a diffusion controlled phenomenon. Diameter of the semi-circle is called charge-transfer resistance or impedance (R_{CT}). Higher the value of R_{CT}, lower is the conductivity of the specific electrode and vice versa [37–39]. EIS analysis of unmodified GCE and *GCE/Chit-fCNT* were carried out and the results were expressed in the form of Nyquist and Bode plots (Fig. 4).

The R_{CT} value for bare GCE is as high as 2340 Ω, whereas for *GCE/Chit-fCNT* electrode the R_{CT} became almost negligible. The Nyquist plot of *GCE/Chit-fNCT* displayed only the diffusion controlled phenomenon without any charge transfer resistance. The response of phase angle as well as impedance with varying frequency can be represented in the form of Bode plot of EIS data. In both the cases of bare and modified GCE, the phase angle maximum indicates the electrode nature as uniform all over the surface, whereas impedance response reveals that the *GCE/Chit-fCNT* has very low impedance values compared to bare GCE. It could be attributed to the high conductivity of *fCNT* and its fine dispersion in the nanocomposite film. It is also observed that there is a

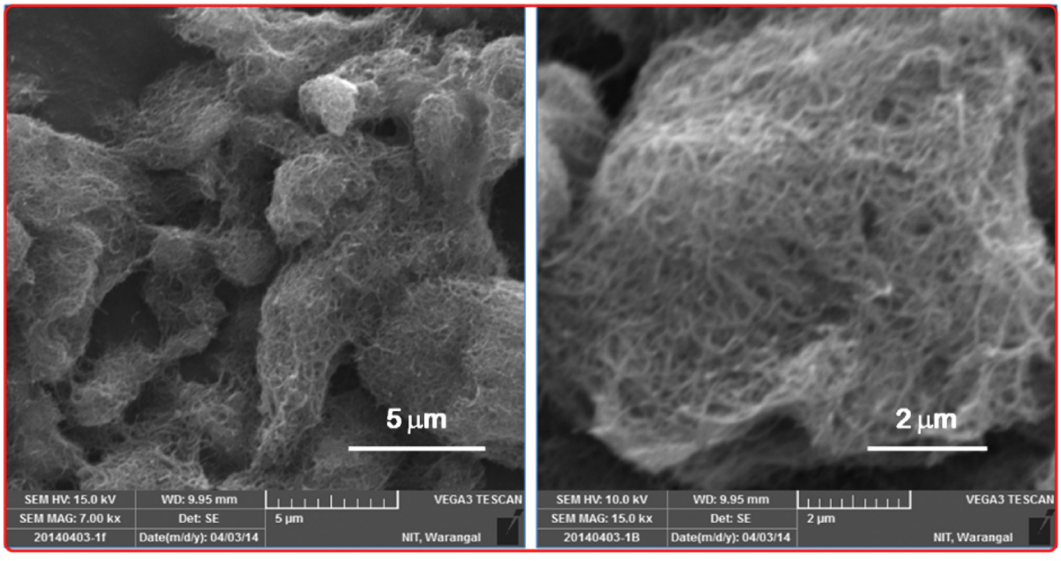

Fig. 2. SEM images of *Chit-fCNT* nanocomposite film at two different magnifications.

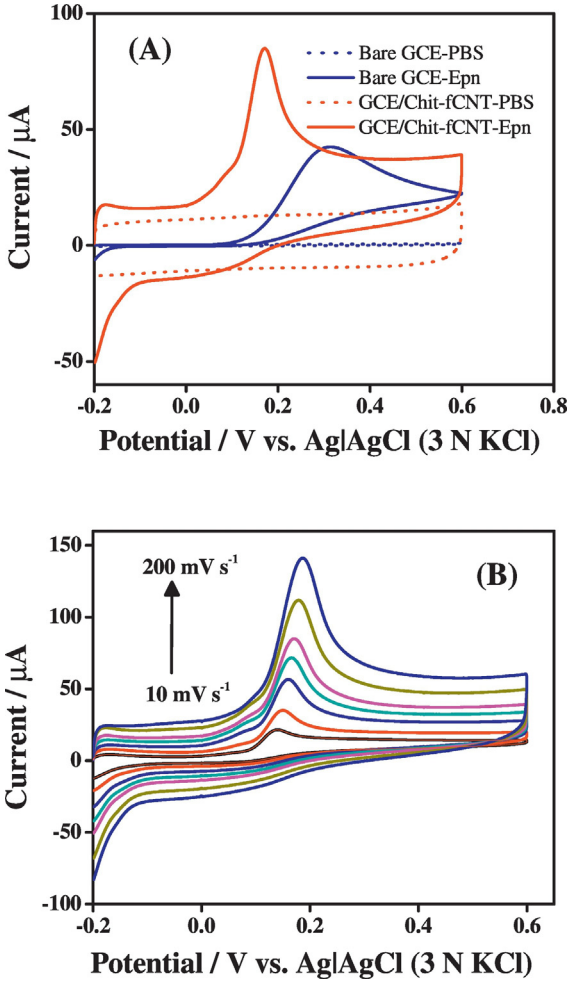

Fig. 3. (A) CV response of bare GCE and *GCE/Chit-fCNT* in the presence and absence of 0.1 mM epinephrine in 50 mM PBS (pH 7.4) at 100 mV s^{-1}. (B) CVs of 0.1 mM epinephrine at *GCE/Chit-fCNT* with various scan rates 10, 25, 50, 75, 100, 150 and 200 mV s^{-1}.

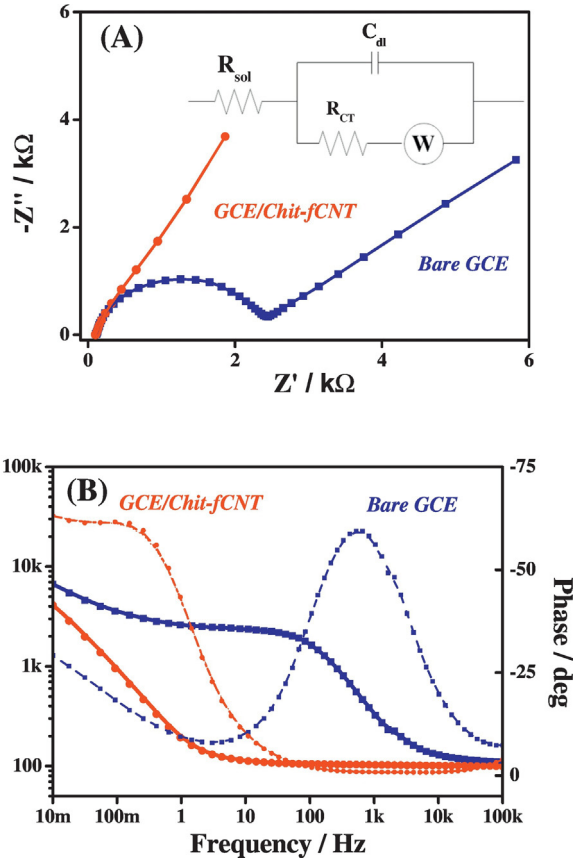

Fig. 4. EIS response in the form of (A) Nyquist and (B) Bode plots of bare GCE and *GCE/Chit-fCNT* in an aq. 1 mM $K_3[Fe(CN)_6]$ + 0.1 M KCl. Inset: Randles equivalent circuit.

high diffusion of redox molecules towards the *GCE/Chit-fCNT* (Fig. 4(B)), which indicates the high surface area of the *Chit-fCNT* composite film. From the EIS data, we can conclude that the *Chit-fCNT* nanocomposite film allows greater permeation of analyte molecules and efficient electron transfer process [40].

Results of all these SEM, CV and EIS investigations put together clearly infer that the hybrid nanocomposite *Chit-fCNT* promoted electron-transfer across the interface and thermodynamically reduced the overpotential for Epn oxidation. The observed results could necessarily be attributed to the porous surface morphology, the interconnecting threadlike network of highly conducting carbon nanotubes and the biocompatible chitosan polymer matrix embedded them.

3.5. Voltammetric detection of epinephrine

The fabricated *GCE/Chit-fCNT* electrode was employed for voltammetric detection of Epn by DPV analysis. Very good voltammetric peak response of Epn was observed at 0.1 V with the optimized parameters of 20 mV s^{-1} scan rate, 100 mV pulse amplitude, 0.2 s pulse period and 10 mV increment. With the optimized parameters, differential pulse voltammetric analysis was carried out with varying concentrations of Epn in PBS buffer in the determination range of 0–10 µM (Fig. 5(A)). Calibration plot has been drawn with the observed peak current vs. Epn concentration (Fig. 5(B)).

Low detection limit of the fabricated sensor has been evaluated from the DPV results by using the formula "$3\sigma/b$", where 'σ' indicates the RSD of the oxidation peak currents of Epn in three successive measurements and 'b' represents slope of the calibration plot. A low-detection-limit of 30 nM was established with a linear determination range of 0.05–10 µM Epn. The experimental results obtained using the present fabricated sensor system have been compared with the other analytical methods and electrochemical sensor systems reported in the literature (Table 1). Determination of Epn by UPLC-MS/MS method combining reductive ethylation labeling and protein precipitation technique exhibited a very low-detection-limit of 0.1×10^{-9} M [2]. A capillary electrophoresis determination employing CdTe quantum dots for enhancing chemiluminescence exhibited a low-detection-limit of 9.0×10^{-9} M [4]. DPV detection of epinephrine at an overoxidized polypyrrole film comprised of Au nanoclusters demonstrated a low-detection-limit of 3.0×10^{-8} M [41]. Electrochemical determination of epinephrine by DPV analysis using poly(serine) modified CNT electrode demonstrated a low-detection-limit of 6.0×10^{-7} M [42]. The low-detection-limit of the present electochemical sensor employing a biocompatible chitosan polymer based CNT electrode is 3.0×10^{-8} M and is highly comparable to the detection limits reported earlier employing different modified electrodes. The analysis time for the detection of Epn is below 10 s, and the electrochemical analysis could easily be tailored to on-site analysis with miniature instruments and automated flow-injection analysis system. Further investigations for direct analysis of Epn from physiological samples could be carried out, as the levels of Epn in healthy human lies in nanomolar level [7]. Thus, interference studies were carried out to ascertain the selectivity of present sensor system towards the detection of Epn. Further, the modified electrode was tested for the specific detection of Epn from pharmaceutical injections and artificial urine samples.

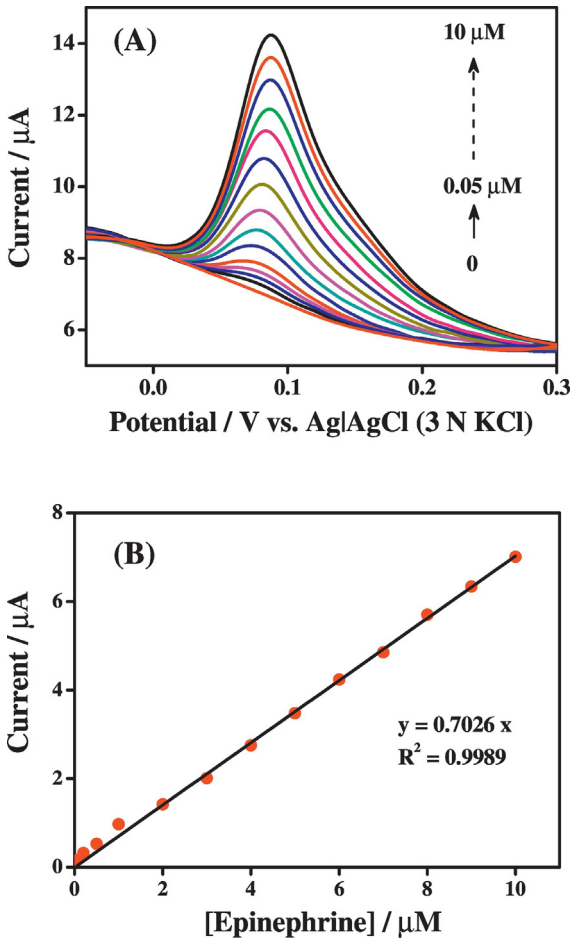

Fig. 5. (A) DPV responses of epinephrine recorded at different concentrations (0–10 μM) in PBS at *GCE/Chit-fCNT*. (B) Calibration plot of peak current vs. epinephrine concentration.

3.6. Interference studies

The fabricated sensor was tested towards the voltammetric detection of Epn despite the coexistence of potential electroactive biomolecules, e.g. ascorbic acid (AA), uric acid (UA) and serotonin (Ser). DPV analysis was carried out at both bare GCE and *GCE/Chit-fCNT* in a mixture of 5 μM each of AA, UA and Ser with varying concentrations of Epn (4, 6, 8 and 10 μM) and are shown in Fig. 6. The mixture of Epn, AA, UA and Ser exhibited only a single broad peak with a very poor current response at bare GCE, whereas four distinct characteristic peaks were observed at the fabricated *GCE/Chit-fCNT* (Fig. 6A). The anodic current response of Epn at the *GCE/Chit-fCNT* enhanced steadily with an increase in Epn concentration despite the presence of a mixture of interferents (Fig. 6B), and distinction of the peaks was maintained between these interferents and Epn. Experimental data revealed that the nanocomposite electrode worked efficiently for the selective voltammetric detection of Epn and can be applied successfully for real time analysis of Epn in the coexistence of potential biological interferents.

3.7. Repeatability and reproducibility

The fabricated sensor system has been examined for reproducibility of the results in the DPV analysis of 10 μM Epn repetitively using a same electrode. In complete span of a week, the fabricated electrode was tested for ~25 times in DPV measurements of Epn, which exhibited results with only a very low variation of ~4.5% in the voltammetric current response. Further, the oxidation peak potential of individual electrodes did not vary during the analyses for one month period, if it stored in PBS when not in use. These experimental results reveal the stability and repeatability of the modified electrode. Further, standard deviation of the peak currents for 10 μM Epn in multiple experiments with a number of electrodes fabricated independently ($n = 6$) was merely 2.5%, which infers the excellent reproducibility of the demonstrated sensor system. These experimental results revealed that the *Chit-fCNT* composition formed a reproducible and stable electroactive bio-nanocomposite film on GCE surface.

3.8. Direct detection of epinephrine in artificial urine and pharmaceutical injections

Voltammetric detection of Epn was carried out in artificial urine and in pharmaceutical injections using *GCE/Chit-fCNT* by applying DPV method. DPV response of Epn was analyzed to calculate the recovery limits for the amount of Epn added into artificial urine samples. In the absence of Epn i.e. in the artificial urine alone, the fabricated electrode did not show any characteristic peak. But, the addition of Epn resulted

Table 1
Low-detection-limits and determination ranges for epinephrine by electrochemical, chemiluminescence and chromatographic methods.

Method	Features description	Real sample analysis	Interferents overcame	Linear range (M)	Limit of detection (M)	Ref
UPLC-MS/MS	Labeling with ethylation	Plasma samples	–	0.2×10^{-9}–1.4×10^{-7} (0.05–25 ng mL^{-1})	0.1×10^{-9} (0.025 ng mL^{-1})	[2]
Capillary electrophoresis	CdTe quantum dot enhanced chemiluminescence	Human urine samples	–	4.0×10^{-8}–5.0×10^{-6}	9.0×10^{-9}	[4]
Chemiluminescence	Preconcentration with MIP	Serum samples	–	5.0×10^{-9}–1.0×10^{-7}	3.0×10^{-9}	[7]
Electrochemiluminescence		Pharmaceutical samples	–	4.0×10^{-8}–2.0×10^{-7}	2.4×10^{-8}	[5]
DPV	Poly(serine)	Pharmaceutical injections and Serum	EP, Ser, FA	1.0×10^{-6}–2.2×10^{-4}	6.0×10^{-7}	[42]
DPV	Poly(p-xylenolsulfone-phthalein)	Urine and pharmaceutical samples	AA, UA	2.0×10^{-6}–3.9×10^{-4}	0.1×10^{-6}	[43]
DPV	Polypyrrole/MWCNT composite	Synthetic serum and pharmaceutical samples	AA, UA	0.1×10^{-6}–1.0×10^{-4}	4.0×10^{-8}	[44]
DPV	NanoAu-TiO_2/CNT-rGO	Urine and pharmaceutical samples	AA, UA	1.0×10^{-9}–3.0×10^{-7}	0.3×10^{-9}	[45]
DPV	NanoAu on polypyrrole	Urine and pharmaceutical samples	AA, UA	0.3×10^{-6}–2.1×10^{-5}	3.0×10^{-8}	[41]
DPV	NanoNi$(OH)_2$/CNT	Diluted urine samples	Piroxicam, AA, UA	1.0×10^{-6}–2.2×10^{-4}	2.9×10^{-7}	[46]
Amperometry	Nanoparticles of Pd-Au	–	AA, Glucose	5.0×10^{-6}–2.6×10^{-4}	5.0×10^{-6}	[47]
DPV	*Chit-fCNT* bio-nanocomposite	Artificial urine and pharmaceutical samples	AA, UA, Ser	5.0×10^{-8}–1.0×10^{-5}	3.0×10^{-8}	Present work

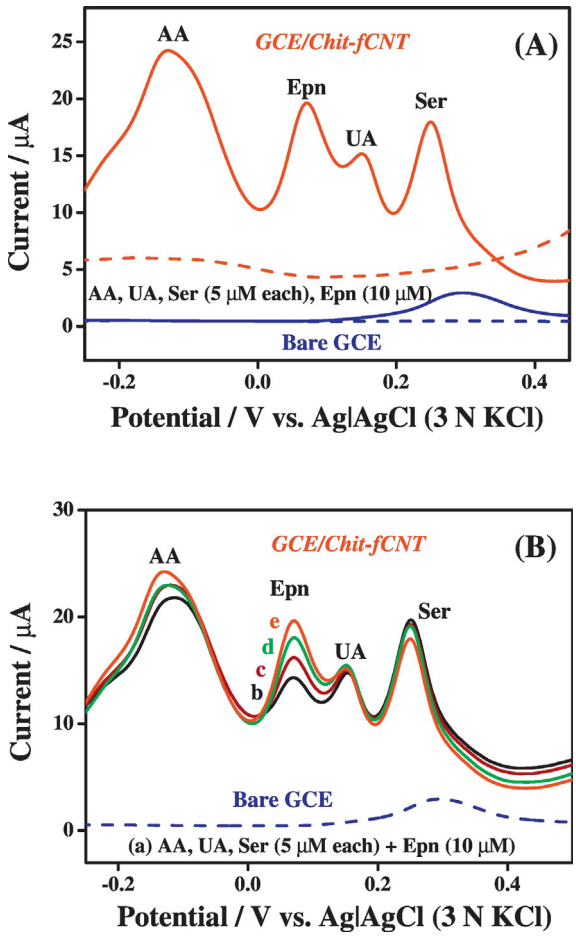

Fig. 6. (A) DPVs of bare and modified GCE in the absence (dotted lines) and presence (full lines) of a mixture of AA, UA and Ser 5 μM each and Epn 10 μM in PBS (pH = 7.4). (B) DPVs of bare (a) and modified GCE (b–e) in PBS (pH = 7.4) containing a mixture of AA, UA and Ser 5 μM each along with epinephrine at different concentrations 4 (b), 6 (c), 8 (d), 10 (a, e) μM.

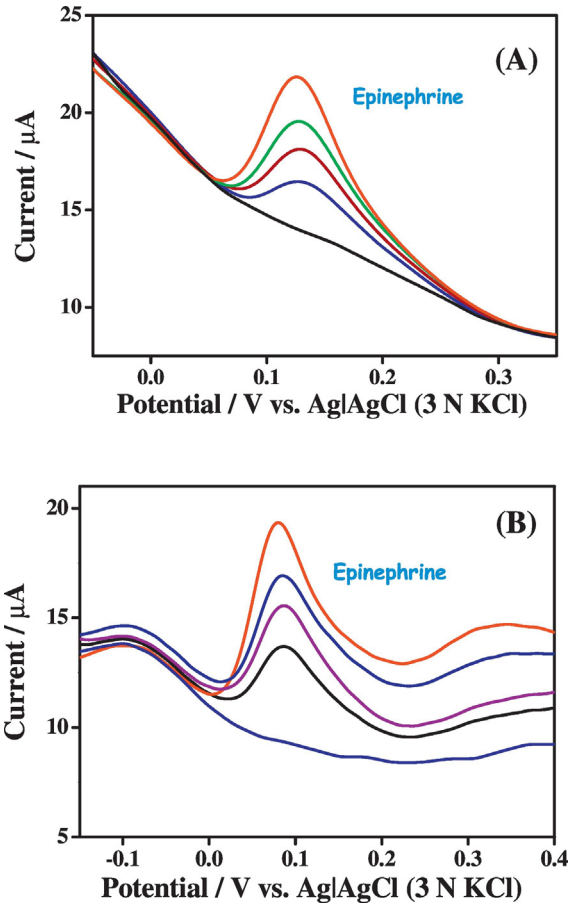

Fig. 7. DPVs of epinephrine of various concentrations (0, 4, 6, 8, 12 μM) at *GCE/Chit-fCNT* (A) in artificial urine (pH = 7.4) and (B) in Adrenaline bitartrate injections (Vasocon) in PBS.

a well-defined oxidation peak (Fig. 7(A)), indicating the efficiency and selective response of the fabricated electrode for the direct detection of Epn from urine samples even at very low concentrations (4 to 12 μM). The recovery limits for the addition of Epn at 4 to 12 μM concentrations varied from 95.7% to 102.1%. Similarly, DPV analysis was carried out for Epn determination directly from pharmaceutical injection samples. The peak current of Epn observed for the addition of adrenaline bitartrate injections in different amounts was monitored (Fig. 7(B)). The recovery limits for the addition of 4 to 12 μM Epn of the pharmaceutical sample varied from 96.5% to 105.6% and the observed results have been compiled in Table 2. All these observations clearly reveal that the present *fCNT*-based nano-biocomposite can be applied effectively for the direct detection of Epn from artificial urine and pharmaceutical adrenaline injections.

4. Conclusions

An efficient and highly sensitive biosensor was fabricated for the selective detection of Epn at physiological pH. With the fabricated *GCE/Chit-fCNT* electrode, DPVs of Epn showed an oxidation peak at reduced overpotentials. Low detection limit of Epn achieved as low as 30 nM with the linear concentration range of 0.05–10 μM. With the unique binding characteristic of Chit biopolymer, a highly stable nanocomposite film capable of multiple analyses over a long period of time was achieved. The fabricated electrode was efficient for the detection of epinephrine selectively despite the coexistence of various potential biological interferents, and it exhibited very good recovery limits for direct determination from urine and adrenaline injection samples. Good reproducibility, reusability and high recovery limits combined with the reliable and easy fabrication protocols of the present sensor system make the CNT based electrodes coupled with the chitosan biopolymer promising for further explorations of biosensors for pharmaceutical compounds.

Acknowledgements

KKR and HK acknowledge deeply the support received from National Research Foundation of Korea (NRF) - Grants funded by the Ministry of Education (2009-0093816), Republic of Korea. S, YG and KVG

Table 2
Recognition of epinephrine in artificial urine and adrenaline injections at the developed *GCE/Chit-fCNT*.

Sample	Epinephrine ($\times 10^{-6}$ M)		Recovery (%)	[a]RSD (%)
	Added	[a]Found		
Urine sample	4.00	3.87	96.9	1.3
	6.00	6.07	101.1	0.7
	8.00	8.17	102.1	0.9
	12.00	11.48	95.7	1.7
Adrenaline injections (Vasocon)	4.00	4.05	105.6	1.3
	6.00	6.24	96.5	1.6
	8.00	7.71	94.6	2.6
	12.00	12.48	104.0	0.9

[a] Measured six times for calculating the mean value.

acknowledge the Ministry of Human Resource Development, India and National Institute of Technology Warangal, India for Doctoral Research Fellowship and for the financial support.

References

[1] P. Hernández, I. Sánchez, F. Patón, L. Hernández, Cyclic voltammetry determination of epinephrine with a carbon fiber ultramicroelectrode, Talanta 46 (1998) 985–991, http://dx.doi.org/10.1016/S0039-9140(97)00353-6.

[2] C. Ji, J. Walton, Y. Su, M. Tella, Simultaneous determination of plasma epinephrine and norepinephrine using an integrated strategy of a fully automated protein precipitation technique, reductive ethylation labeling and UPLC-MS/MS, Anal. Chim. Acta 670 (2010) 84–91, http://dx.doi.org/10.1016/j.aca.2010.04.051.

[3] N.F. Atta, A. Galal, E.H. El-Ads, A novel sensor of cysteine self-assembled monolayers over gold nanoparticles for the selective determination of epinephrine in presence of sodium dodecyl sulfate, Analyst 137 (2012) 2658–2668, http://dx.doi.org/10.1039/c2an16210e.

[4] Y. Zhao, S. Zhao, J. Huang, F. Ye, Quantum dot-enhanced chemiluminescence detection for simultaneous determination of dopamine and epinephrine by capillary electrophoresis, Talanta 85 (2011) 2650–2654, http://dx.doi.org/10.1016/j.talanta.2011.08.032.

[5] Y. Su, J. Wang, G. Chen, Determination of epinephrine based on its enhancement for electrochemiluminescence of lucigenin, Talanta 65 (2005) 531–536, http://dx.doi.org/10.1016/j.talanta.2004.07.015.

[6] F.D.P. Ferreira, L.I.B. Silva, A.C. Freitas, T.A.P. Rocha-Santos, A.C. Duarte, High performance liquid chromatography coupled to an optical fiber detector coated with laccase for screening catecholamines in plasma and urine, J. Chromatogr. A 1216 (2009) 7049–7054, http://dx.doi.org/10.1016/j.chroma.2009.08.067.

[7] J. Du, L. Shen, J. Lu, Flow injection chemiluminescence determination of epinephrine using epinephrine-imprinted polymer as recognition material, Anal. Chim. Acta 489 (2003) 183–189, http://dx.doi.org/10.1016/S0003-2670(03)00717-7.

[8] H. Gu, X. Di Su, K.P. Loh, Electrochemical impedance sensing of DNA hybridization on conducting polymer film-modified diamond, J. Phys. Chem. B 109 (2005) 13611–13618, http://dx.doi.org/10.1021/jp050625p.

[9] X. Yang, B. Feng, X. He, F. Li, Y. Ding, J. Fei, Carbon nanomaterial based electrochemical sensors for biogenic amines, Microchim. Acta 180 (2013) 935–956, http://dx.doi.org/10.1007/s00604-013-1015-6.

[10] S. Shahrokhian, M. Ghalkhani, M.K. Amini, Application of carbon-paste electrode modified with iron phthalocyanine for voltammetric determination of epinephrine in the presence of ascorbic acid and uric acid, Sensors Actuators B Chem. 137 (2009) 669–675, http://dx.doi.org/10.1016/j.snb.2009.01.022.

[11] W. Ren, H.Q. Luo, N.B. Li, Simultaneous voltammetric measurement of ascorbic acid, epinephrine and uric acid at a glassy carbon electrode modified with caffeic acid, Biosens. Bioelectron. 21 (2006) 1086–1092, http://dx.doi.org/10.1016/j.bios.2005.04.002.

[12] J. Kirsch, C. Siltanen, Q. Zhou, A. Revzin, A. Simonian, Biosensor technology: recent advances in threat agent detection and medicine, Chem. Soc. Rev. 42 (2013) 8733–8768, http://dx.doi.org/10.1039/c3cs60141b.

[13] C. Dhand, N. Dwivedi, X.J. Loh, A.N. Jie Ying, N.K. Verma, R.W. Beuerman, R. Lakshminarayanan, S. Ramakrishna, Methods and strategies for the synthesis of diverse nanoparticles and their applications: a comprehensive overview, RSC Adv. 5 (2015) 105003–105037, http://dx.doi.org/10.1039/C5RA19388E.

[14] E. Ye, M.D. Regulacio, M.S. Bharathi, H. Pan, M. Lin, M. Bosman, K.Y. Win, H. Ramanarayan, S.-Y. Zhang, X.J. Loh, Y.-W. Zhang, M.-Y. Han, An experimental and theoretical investigation of the anisotropic branching in gold nanocrosses, Nanoscale. 8 (2016) 543–552, http://dx.doi.org/10.1039/C5NR07182H.

[15] R. Lakshminarayanan, X.J. Loh, S. Gayathri, S. Sindhu, Y. Banerjee, R.M. Kini, S. Valiyaveettil, Formation of transient amorphous calcium carbonate precursor in quail eggshell mineralization: an in vitro study, Biomacromolecules 7 (2006) 3202–3209, http://dx.doi.org/10.1021/bm0605412.

[16] X.J. Loh, T.-C. Lee, Q. Dou, G.R. Deen, Utilising inorganic nanocarriers for gene delivery, Biomater. Sci. 4 (2016) 70–86, http://dx.doi.org/10.1039/C5BM00277J.

[17] Z. Li, E. Ye, David, R. Lakshminarayanan, X.J. Loh, Recent advances of using hybrid nanocarriers in remotely controlled therapeutic delivery, Small 12 (2016) 4782–4806, http://dx.doi.org/10.1002/smll.201601129.

[18] E. Ye, X.J. Loh, Polymeric hydrogels and nanoparticles: a merging and emerging field, Aust. J. Chem. 66 (2013) 997, http://dx.doi.org/10.1071/CH13168.

[19] K. Huang, Q. Dou, X.J. Loh, Nanomaterial mediated optogenetics: opportunities and challenges, RSC Adv. 6 (2016) 60896–60906, http://dx.doi.org/10.1039/C6RA11289G.

[20] H.C. Guo, E. Ye, Z. Li, M.-Y. Han, X.J. Loh, Recent progress of atomic layer deposition on polymeric materials, Mater. Sci. Eng. C 70 (2017) 1182–1191, http://dx.doi.org/10.1016/j.msec.2016.01.093.

[21] X.J. Loh, Q.Q. Dou, E. Ye, C.P. Teng, Effective near-infrared photodynamic therapy assisted by upconversion nanoparticles conjugated with photosensitizers, Int. J. Nanomedicine 10 (2015) 419–432, http://dx.doi.org/10.2147/IJN.S74891.

[22] K. Koteshwara Reddy, K. Vengatajalabathy Gobi, Activated direct electron transfer of nanoAu bioconjugates of cytochrome c for electrocatalytic detection of trace levels of superoxide dismutase enzyme, Electrochim. Acta 78 (2012) 109–114, http://dx.doi.org/10.1016/j.electacta.2012.05.159.

[23] R. Lakshminarayanan, E.O. Chi-Jin, X.J. Loh, R.M. Kini, S. Valiyaveettil, Purification and characterization of a vaterite-inducing peptide, pelovaterin, from the eggshells of *Pelodiscus sinensis* (Chinese Soft-Shelled Turtle), Biomacromolecules 6 (2005) 1429–1437, http://dx.doi.org/10.1021/bm049276f.

[24] B.M. Teo, D.J. Young, X.J. Loh, Magnetic anisotropic particles: toward remotely actuated applications, Part. Part. Syst. Charact. 33 (2016) 709–728, http://dx.doi.org/10.1002/ppsc.201600060.

[25] Q. Dou, X. Fang, S. Jiang, P.L. Chee, T.-C. Lee, X.J. Loh, Multi-functional fluorescent carbon dots with antibacterial and gene delivery properties, RSC Adv. 5 (2015) 46817–46822, http://dx.doi.org/10.1039/C5RA07968C.

[26] X. Wu, X. Chen, J. Wang, J. Liu, Z. Fan, X. Chen, J. Chen, Functionalization of multiwalled carbon nanotubes with thermotropic liquid-crystalline polymer and thermal properties of composites, Ind. Eng. Chem. Res. 50 (2011) 891–897, http://dx.doi.org/10.1021/ie1018029.

[27] M.E. Ghica, C.M.A. Brett, Simple and efficient epinephrine sensor based on carbon nanotube modified carbon film electrodes, Anal. Lett. 46 (2013) 1379–1393, http://dx.doi.org/10.1080/00032719.2012.762584.

[28] T. Brooks, C.W.W. Keevil, A simple artificial urine for the growth of urinary pathogens, Lett. Appl. Microbiol. 24 (1997) 203–206, http://dx.doi.org/10.1046/j.1472-765X.1997.00378.x.

[29] X. Lu, W.-L. Yim, B.H.R. Suryanto, C. Zhao, Electrocatalytic oxygen evolution at surface-oxidized multiwall carbon nanotubes, J. Am. Chem. Soc. 137 (2015) 2901–2907, http://dx.doi.org/10.1021/ja509879r.

[30] C.H. An Wong, M. Pumera, C. Hong, A. Wong, Highly conductive graphene nanoribbons from the reduction of graphene oxide nanoribbons with lithium aluminium hydride, J. Mater. Chem. C 2 (2014) 856–863, http://dx.doi.org/10.1039/c3tc31688b.

[31] E. Nossol, A.J. Gorgatti Zarbin, Transparent films from carbon nanotubes/Prussian blue nanocomposites: preparation, characterization, and application as electrochemical sensors, J. Mater. Chem. 22 (2012) 1824–1833, http://dx.doi.org/10.1039/c1jm14225a.

[32] P. Li, Y. Ding, A. Wang, L. Zhou, S. Wei, Y. Zhou, Y. Tang, Y. Chen, C. Cai, T. Lu, Self-assembly of tetrakis (3-trifluoromethylphenoxy) phthalocyaninato cobalt(II) on multiwalled carbon nanotubes and their amperometric sensing application for nitrite, ACS Appl. Mater. Interfaces 5 (2013) 2255–2260, http://dx.doi.org/10.1021/am400152k.

[33] J. Fan, Z. Shi, M. Tian, J. Wang, J. Yin, Unzipped multiwalled carbon nanotube oxide/multiwalled carbon nanotube hybrids for polymer reinforcement, ACS Appl. Mater. Interfaces 4 (2012) 5956–5965, http://dx.doi.org/10.1021/am301623t.

[34] L.G. Bulusheva, A.V. Okotrub, I.A. Kinloch, I.P. Asanov, A.G. Kurenya, A.G. Kudashov, X. Chen, H. Song, Effect of nitrogen doping on Raman spectra of multi-walled carbon nanotubes, Phys. Status Solidi 245 (2008) 1971–1974, http://dx.doi.org/10.1002/pssb.200879592.

[35] M. Satyanarayana, K. Koteshwara Reddy, K. Vengatajalabathy Gobi, Nanobiocomposite based electrochemical sensor for sensitive determination of serotonin in presence of dopamine, ascorbic acid and uric acid in vitro, Electroanalysis 26 (2014) 2365–2372, http://dx.doi.org/10.1002/elan.201400243.

[36] M. Satyanarayana, K.K. Reddy, K.V. Gobi, Multiwall carbon nanotube ensembled biopolymer electrode for selective determination of isoniazid in vitro, Anal. Methods 6 (2014) 3772–3778, http://dx.doi.org/10.1039/c4ay00154k.

[37] E.P. Randviir, C.E. Banks, Electrochemical impedance spectroscopy: an overview of bioanalytical applications, Anal. Methods 5 (2013) 1098–1115, http://dx.doi.org/10.1039/c3ay26476a.

[38] A. Bogomolova, E. Komarova, K. Reber, T. Gerasimov, O. Yavuz, S. Bhatt, M. Aldissi, Challenges of electrochemical impedance spectroscopy in protein biosensing, Anal. Chem. 81 (2009) 3944–3949, http://dx.doi.org/10.1021/ac9002358.

[39] B. Pejcic, R. De Marco, Impedance spectroscopy: over 35 years of electrochemical sensor optimization, Electrochim. Acta 51 (2006) 6217–6229, http://dx.doi.org/10.1016/j.electacta.2006.04.025.

[40] I.I. Suni, Impedance methods for electrochemical sensors using nanomaterials, TrAC Trends Anal. Chem. 27 (2008) 604–611, http://dx.doi.org/10.1016/j.trac.2008.03.012.

[41] J. Li, X. Lin, Electrodeposition of gold nanoclusters on overoxidized polypyrrole film modified glassy carbon electrode and its application for the simultaneous determination of epinephrine and uric acid under coexistence of ascorbic acid, Anal. Chim. Acta 596 (2007) 222–230, http://dx.doi.org/10.1016/j.aca.2007.05.057.

[42] P.V. Narayana, T. Madhusudana Reddy, P. Gopal, M. Mohan Reddy, G. Ramakrishna Naidu, Electrocatalytic boost up of epinephrine and its simultaneous resolution in the presence of serotonin and folic acid at poly(serine)/multi-walled carbon nanotubes composite modified electrode: a voltammetric study, Mater. Sci. Eng. C 56 (2015) 57–65, http://dx.doi.org/10.1016/j.msec.2015.06.011.

[43] A.A. Ensafi, M. Taei, T. Khayamian, Simultaneous determination of ascorbic acid, epinephrine, and uric acid by differential pulse voltammetry using poly(p-xylenolsulfonephthalein) modified glassy carbon electrode, Colloids Surf. B: Biointerfaces 79 (2010) 480–487, http://dx.doi.org/10.1016/j.colsurfb.2010.05.017.

[44] S. Shahrokhian, R. Saberi, Electrochemical preparation of over-oxidized polypyrrole/multi-walled carbon nanotube composite on glassy carbon electrode and its application in epinephrine determination, Electrochim. Acta 57 (2011) 132–138, http://dx.doi.org/10.1016/j.electacta.2011.04.029.

[45] J. Li, X. Wang, H. Duan, Y. Wang, C. Luo, Ultra-sensitive determination of epinephrine based on TiO2-Au nanoclusters supported on reduced graphene oxide and carbon nanotube hybrid nanocomposites, Mater. Sci. Eng. C 64 (2016) 391–398, http://dx.doi.org/10.1016/j.msec.2016.04.003.

[46] A. Babaei, M. Sohrabi, M. Afrasiabi, A sensitive simultaneous determination of epinephrine and piroxicam using a glassy carbon electrode modified with a nickel hydroxide nanoparticles/multiwalled carbon nanotubes composite, Electroanalysis 24 (2012) 2387–2394, http://dx.doi.org/10.1002/elan.201200483.

[47] T.-H. Tsai, S. Thiagarajan, S.-M. Chen, C.-Y. Cheng, Ionic liquid assisted synthesis of nano Pd–Au particles and application for the detection of epinephrine, dopamine and uric acid, Thin Solid Films 520 (2012) 3054–3059, http://dx.doi.org/10.1016/j.tsf.2011.11.005.